RSC Advances

PAPER

View Article Online
View Journal | View Issue

Cite this: *RSC Adv.*, 2024, **14**, 35618

Harnessing the UiO-67 metal–organic framework for advanced detection of cadmium ions in water bodies

Bhuvaneswari Selvaraj,[ab] Lakshmi Priya G. *[ac] and Selva Balasubramanian[de]

Received 21st September 2024
Accepted 29th October 2024

DOI: 10.1039/d4ra06811d

rsc.li/rsc-advances

Heavy metal ions are hazardous pollutants that pose serious threats to ecosystems and human health, making it imperative to detect and monitor their presence in water for environmental protection. This paper highlights the synthesis of the UiO-67 Metal–Organic Framework (MOF) without any dopants, offering a novel approach specifically for the detection of cadmium ions (Cd^{2+}) in aqueous environments. Following solvothermal synthesis, Powder X-ray Diffraction (PXRD), BET nitrogen adsorption–desorption analysis, X-ray Photoelectron Spectroscopy (XPS), and Scanning Electron Microscopy (SEM) were used to characterize the structural and morphological features of UiO-67. The MOF exhibited a high pore volume and surface area, which are essential for enhancing its detection capabilities for Cd^{2+} ions. Based on experimental findings, the proposed sensor exhibits excellent selectivity towards Cd^{2+} ions and a sensitivity of 3.008 μA nM^{-1}. Further, it achieves a low Limit of Detection (LoD) of 1.43 nM μA^{-1} and a Limit of Quantification (LoQ) of 4.34 nM μA^{-1}. The sensitivity and reliability of the UiO-67-modified electrode are demonstrated by these values, which qualify it for trace-level cadmium ion detection. The ground-breaking potential of undoped UiO-67 serves as a cutting-edge and effective tool for environmental monitoring, particularly in the detection of toxic metal ions in water bodies.

1. Introduction

Environmental monitoring plays a crucial role in identifying and measuring contaminants that affect water, soil, and air quality.[1] As the global demand for clean, potable water continues to rise, the need for accurate and continuous monitoring of water quality has become increasingly important. The emergence of new pollution sources, driven by industrialization and urbanization, poses significant threats to water resources.[2–4] Among the most critical environmental challenges is Heavy Metal Ion (HMI) pollution, which presents a serious risk to global sustainability due to its nonbiodegradable and highly toxic nature.[5–7]

Heavy metal ions, including cadmium (Cd), copper (Cu), lead (Pb), arsenic (As),[8] and mercury (Hg), are among the most dangerous pollutants found in water systems.[9–11] These metals primarily enter the environment through human activities, including industrial emissions, mining operations, and the application of pesticides. Once introduced, they can persist in ecosystems for extended periods. Their accumulation in the food chain results in bio-magnification, leading to increasingly higher concentrations of these toxic metals in organisms at the top of the food chain, including humans.[7] This poses significant health risks, as exposure to even low levels of heavy metals can cause severe damage to the immune, renal, nervous, and hematopoietic systems.[5,6] In response to these dangers, global health organizations such as the World Health Organization (WHO) and the Environmental Protection Agency (EPA) have established stringent guidelines on permissible levels of heavy metal ions in drinking water and the environment.[9] Exceeding these limits has been associated with a range of health problems, including neurological disorders, reproductive toxicity, cardiovascular diseases, and an increased risk of cancer.[11,12]

Traditional methods for detecting heavy metals, such as Atomic Absorption Spectroscopy (AAS), mass spectrometry, capillary electrophoresis[13] and Inductively Coupled Plasma – Mass Spectrometry (ICP-MS), have been widely used due to their high sensitivity and accuracy. However, these techniques are often expensive, require complex sample preparation, and are not suitable for rapid, on-site analysis.[14] This has led to exploring alternative approaches that are more cost-effective,

[a]*Centre for Advanced Materials and Innovative Technologies (CAMIT), Vellore Institute of Technology (Chennai Campus), Chennai 600127, India. E-mail: lakshmipriya.g@vit.ac.in*

[b]*School of Advanced Science (SAS), Vellore Institute of Technology (Chennai Campus), Chennai 600127, India*

[c]*School of Electronics Engineering (SENSE), Vellore Institute of Technology (Chennai Campus), Chennai 600127, India*

[d]*Centre for Nanotechnology & Advanced Biomaterials (CeNTAB), SASTRA Deemed University, Thanjavur, Tamil Nadu 613 401, India*

[e]*School of Electrical & Electronics Engineering (SEEE), SASTRA Deemed University Thanjavur, Tamil Nadu 613 401, India*

portable, and capable of providing quick results. Electrochemical biosensors have gained attention because of their good response, sensitivity and potential for miniaturization.[11,15]

Materials utilised for detecting heavy metal ions encompass Metal–Organic Frameworks (MOFs),[14,16,17] carbon-based materials,[13,15,18] polymers,[19] and nanoparticles.[20] Notably, MOFs have emerged as a highly promising group of materials for environmental monitoring, especially in the detection of heavy metal ions. MOFs are porous, crystalline materials comprised of metal ions coordinated to organic ligands, creating a highly tunable structure with a large surface area and high porosity.[21–23] Among the various MOFs, UiO-67, a zirconium-based framework, has garnered significant attention due to its exceptional chemical stability, large surface area, and versatile functionalization possibilities.

Cavka *et al.*[24] reported the discovery of UiO-66 and UiO-67, two zirconium-based metal–organic frameworks (MOFs) with exceptional chemical and thermal stability. $ZrO_4(OH)_4$ clusters are used as inorganic nodes that are joined to organic linkers in the framework. High stability is achieved by this structure under a variety of circumstances, such as exposure to moisture and high temperatures, which are generally difficult for other MOFs. The study highlights that because of their robustness, these zirconium-based MOFs with high porosity and wide surface areas may find use in environmental sensing, gas storage, and catalysis.[24,25]

A member of the UiO (University of Oslo) family of metal–organic frameworks (MOFs), UiO-67 is made up of zirconium (Zr) ions coordinated with organic linkers. Compared to UiO-66, the structure is more porous and has bigger pore diameters because Zr clusters are used as inorganic nodes and 4,4′-biphenyl dicarboxylate is used as an organic linker. Zr clusters are renowned for their exceptional chemical and thermal stability, which gives UiO-67 exceptional resistance to extreme environmental factors, including high temperatures and acidic or basic environments.[26,27] UiO-67, a zirconium-based metal–organic framework, can be modified in several ways to enhance its performance for different applications.

The basic form of UiO-67 has a high surface area and large pore size, making it ideal for gas adsorption, catalysis, and environmental sensing. It can be functionalized with amine (UiO-67-NH_2), sulfonic acid (UiO-67-SO_3H), or carboxylic acid (UiO-67-COOH) groups to improve interaction with specific molecules, enhance proton conductivity, or boost adsorption efficiency. UiO-67 can also be modified with hydroxyl groups (UiO-67-OH) for increased chemical reactivity or doped with metals such as copper, iron, or nickel to improve catalytic performance. Embedding nanoparticles, like gold (UiO-67-Au) or palladium (UiO-67-Pd), enhances catalytic properties for reactions involving metals. Composites with materials like graphene oxide increase its electrical conductivity, making it suitable for electrochemical applications. UiO-67 can also be combined with ionic liquids to improve gas capture and separation, particularly for CO_2, or functionalized with thiophene to enhance conductivity and catalytic activity in sulfur-related processes. These diverse modifications allow UiO-67 to be tailored for various applications, from environmental monitoring to catalysis and sensing. For a number of bio-related uses, including drug delivery, anti-cancer activity, biosensing, and imaging, Zr-MOFs and their composites have been extensively studied. Functionalization with specific ligands enables UiO-67 to direct its payload to tumour cells, where controlled drug release can be triggered by specific stimuli, such as pH changes or enzyme activity.[28–30]

The properties of UiO-67 are particularly suitable for the adsorption and detection of toxic metal ions in aqueous environments.[16,17,31] Specifically, it's robust structure allows for the incorporation of specific functional groups that can selectively interact with heavy metal ions, enhancing the sensitivity and selectivity of the detection process.[32] The material's high surface area and porosity enhance its ability to effectively capture and concentrate metal ions from water samples, allowing for detection at very low concentrations. This makes UiO-67 an ideal candidate for developing advanced sensors for environmental applications, particularly in scenarios where rapid and accurate detection is critical.[17,33–35]

Previous research on zirconium-based metal–organic frameworks (MOFs), especially UiO-67, has emphasized their potential for environmental applications, such as heavy metal detection, due to their exceptional stability, high surface area, and porous structure. Studies have shown that functionalizing UiO-67 with various groups (*e.g.*, amine, sulfonic acid) or embedding nanomaterials (*e.g.*, gold or palladium nanoparticles) enhances selectivity, sensitivity, and catalytic properties, allowing for specific interactions with target heavy metal ions. These modifications are often applied to improve UiO-67's capacity to capture and detect specific ions in complex environmental settings.[36–38] Also, most previous studies focus on either the structural or catalytic aspects of UiO-67 without fully exploring its electrochemical potential for real-time environmental monitoring at regulatory threshold levels (*e.g.*, EPA and WHO standards).[39,40]

However, despite these advances, there remains a gap in understanding the intrinsic capabilities of undoped, unmodified UiO-67 for heavy metal detection, specifically for cadmium ions. In our proposed work, we uniquely employ undoped UiO-67 without any functional group modifications or nanomaterial incorporation, focusing solely on the inherent properties of this pristine MOF. This approach underscores the powerful adsorption capacity and selectivity that undoped UiO-67 can naturally provide, particularly in electrochemical sensing. By leveraging the intrinsic porosity, surface area, and structural robustness of UiO-67, we aim to demonstrate its efficacy in detecting cadmium ions at trace levels, achieving both low limits of detection (LoD) and quantification (LoQ) without added complexity from functionalization. This undoped approach not only simplifies the sensor fabrication process but also highlights UiO-67's baseline performance, offering a straightforward, cost-effective, and reliable solution for environmental monitoring. Thus, our work fills a critical research gap by showcasing the standalone effectiveness of undoped UiO-67 for trace-level cadmium detection, reaffirming its value as a versatile and robust MOF for environmental sensing applications.

In this context, the current work focuses on the application of UiO-67-based materials for developing electrochemical sensors designed to detect cadmium ions. By harnessing the unique properties of UiO-67, these sensors aim to detect metal ions at concentrations below the safety thresholds established by the EPA and WHO.

2. Materials & methods

2.1. Chemicals

Zirconium chloride ($ZrCl_4$ (purity > 98%), MW: 233.02 g mol^{-1}) was sourced from TCI Chemicals India; glacial acetic acid (CH_3COOH (purity > 99.8%), MW: 58.08 g mol^{-1}) was supplied by CDH India; 4,4′-biphenyl dicarboxylic acid (BPDC (purity > 98%), MW: 242.23 g mol^{-1}) was obtained from TCI Chemicals India; *N*,*N*-dimethylformamide (DMF (purity > 99.5%), MW: 60.05 g mol^{-1}) and acetone (C_3H_6O (purity > 99.5%) MW: 58 g mol^{-1}) were provided by Avra India.

2.2. Synthesis of UiO-67 MOF

To prepare the UiO-67 metal–organic framework, 4 mmol of $ZrCl_4$ was dissolved in 100 mL of *N*,*N*-dimethylformamide (DMF) with a subsequent addition of 10 mL acetic acid and 6 mL deionized water under continuous stirring. The reaction solution was subjected to sonication for 20 min to get a complete and homogeneous reaction mixture. Then, 4 mmol of 4,4′-biphenyl dicarboxylic acid (BPDC) was added to the solution under stirring for an additional 20 min. Afterwards, the solution was transferred to a hot air oven and heated at 120 °C for 24 hours. Once cooled to room temperature, the resulting sample was collected by centrifugation and subsequently washed three times each with DMF and acetone. Finally, the sample was dried under vacuum at 80 °C for 24 h and stored in a container for further use. The schematic representation of the UiO-67 synthesis process is shown in Fig. 1.

2.3. Fabrication of UiO-67 MOF-modified glassy carbon electrode (GCE) electrode

To perform electrochemical sensing, a working electrode, a Glassy Carbon Electrode (GCE) was polished using alumina slurries of various particle sizes (1, 0.3 and 0.05 μm) followed by cleaning with ethanol and distilled water to clean the electrode surface. In parallel, 3 mg of UiO-67 in 0.5 mL of DMF (dimethylformamide) was subjected to sonication for 15 min to achieve a homogeneous and well-dispersed solution of UiO-67 particles. Then, 3 μL volume of the well-dispersed UiO-67 was drop-casted over the GCE surface. The conformal coating of UiO-67 layer was obtained by keeping the drop-casted GCE to dry at room temperature and utilized the same for electrochemical studies.

2.4. Characterization studies

The Powder X-ray Diffraction (PXRD) analysis was carried out using a Bruker D8 ADVANCE system (Germany), allowing for precise determination of crystallographic properties. The morphological features were examined using a Field Emission Scanning Electron Microscope (FESEM, JEOL-6701F, Japan) providing detailed insights into the nanostructure's surface and internal characteristics. To analyze functional groups, a Fourier Transform Infrared Spectrometer (FT-IR, Alpha-T, Bruker, Germany) was employed. Additionally, X-ray Photoelectron Spectroscopy (XPS) was conducted using a K-ALPHA from Thermo Scientific in the UK, facilitating the study of elemental composition and chemical states. The surface area and porosity were assessed with a BET surface area analyzer (ASAP 2020, Micromeritics, USA), while electrochemical and impedance

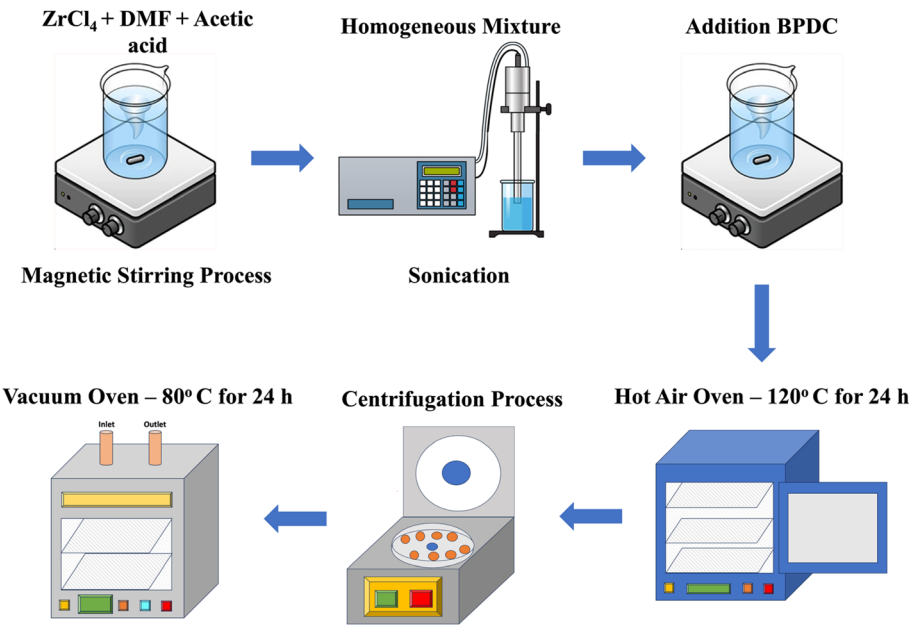

Fig. 1 Schematic representation of UiO-67 synthesis process.

properties were explored using a Squid stat (Admiral Instruments, USA) electrochemical workstation.

3. Results and discussion

3.1. Characteristic features of UiO-67 MOF

Fig. 2(a) displays the powder X-ray diffraction pattern (PXRD) of as-synthesized UiO-67 and the existence of characteristic peaks confirmed the crystallinity and formation of the framework. The observed peaks at 5.8°, 6.7°, 9.1°, 11.0°, 11.6°, 13.3°, 19.6°, 19.9°, 23.8°, 26.6°, and 28.9° correspond to the (111), (002), (022), (113), (222), (004), (133), (024), (006), and (444) crystallographic planes, respectively. This is in good agreement with crystallographic card number 4512073. The consistency of these crystallographic peaks with the existing reports[41] inveterate a well-defined crystalline structure characteristic of the UiO-67 framework.

From Fig. 2(b), it was revealed that UiO-67 crystals have exhibited regular octahedron structure morphology and the existence of corresponding elements (C, O, & Zr) were confirmed from the EDS mapping as shown in Fig. 2(c and d), which is in line with existing report.[42] The estimated atomic percentage of elements is given in the inset of Fig. 2(d).

FTIR spectrum of UiO-67 is presented in Fig. 3(a). The characteristic peaks at 655 and 775 cm^{-1} correspond to Zr–O bonding vibration.[43] The peak centred at 1398 cm^{-1} is due to C=C bonding vibrations of the benzene ring in a ligand moiety.[34] The peaks at 1545 and 1604 cm^{-1} are due to the coordinated carboxylate groups (COO^{-}) in a framework.[44,45] A broad peak at 3422 cm^{-1} is attributed to O–H stretching vibrations, which arise from the hydroxyl groups in water molecules associated with the carboxylate group of BPDC and intercalated water molecules[43,46]

Fig. 3(b) provides the textural properties of the as-synthesized UiO-67, which exhibited a larger surface area of 998 $m^2\ g^{-1}$ and a total pore volume of 0.70 $cm^3\ g^{-1}$. The high nitrogen uptake at pressure (P/P_0 > 0.95) indicates that the

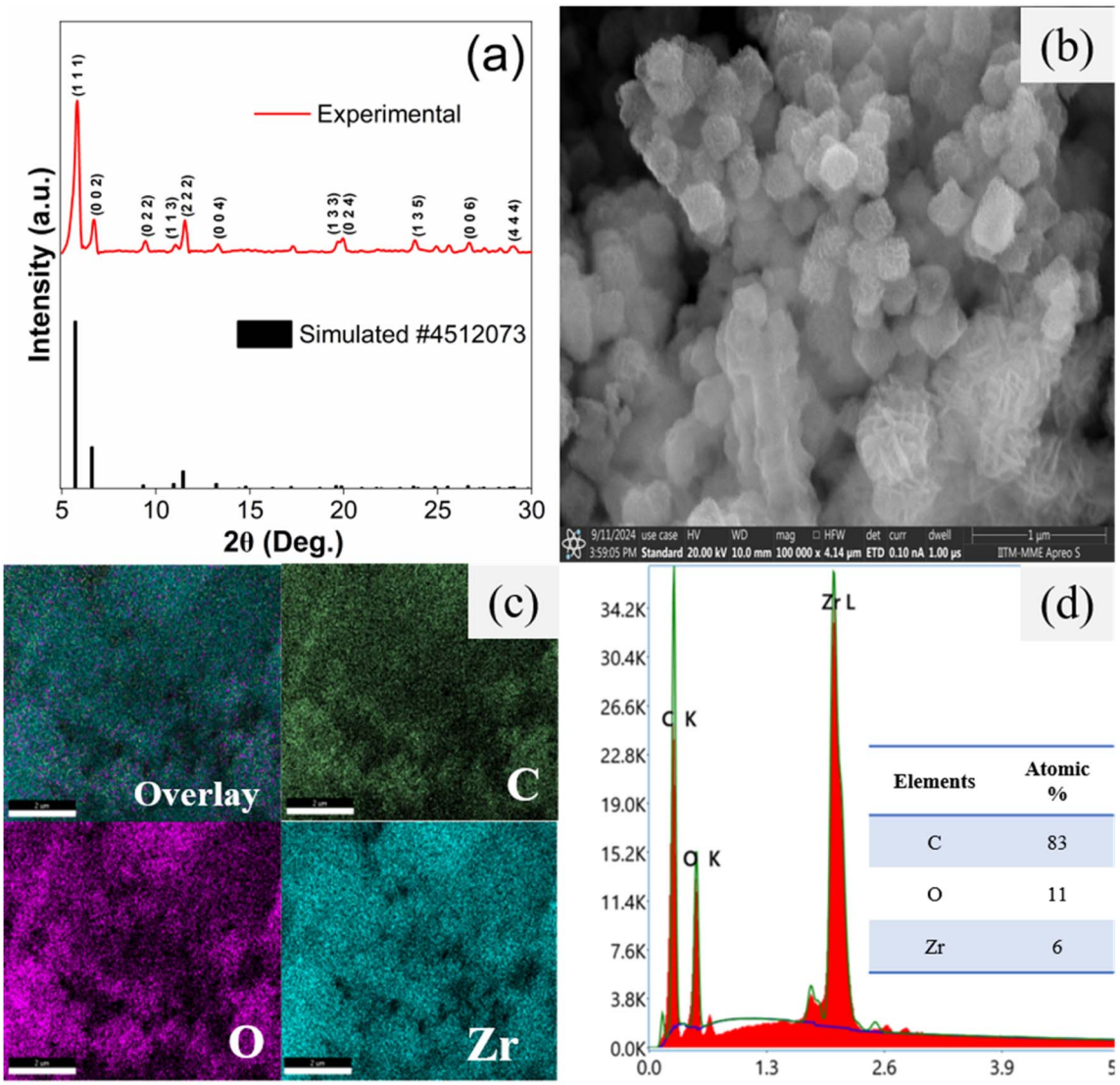

Fig. 2 Structural and morphological studies of UiO-67: (a) PXRD pattern; (b) SEM image; (c) elemental mapping and (d) EDS spectra.

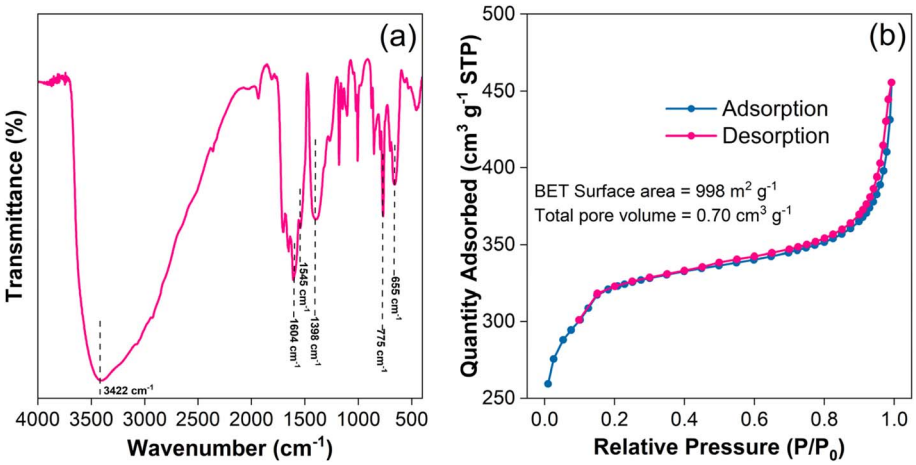

Fig. 3 (a) FTIR spectrum; (b) N_2 isotherm of UiO-67 MOF.

samples follow the Type IV isotherm behaviour.[47] The existence of a hysteresis loop between adsorption and desorption curves revealed the dominance of mesoporosity.[48] Our results demonstrate the material's significant porosity and large surface area, highlighting its potential use for applications that need fine-grained control over pore architecture and a large surface area to enhance performance.

The X-ray photoelectron spectroscopy (XPS) analysis depicted in Fig. 4 offers a detailed examination of the elemental composition and chemical states of UiO-67 framework. As shown in Fig. 4(a), the XPS survey spectra confirm the successful incorporation of zirconium (Zr), oxygen (O), and carbon (C) elements, essential to the material's structure. The Zr 3d spectra in Fig. 4(b) revealed a binding energy separation of 2.35 eV between the Zr $3d_{5/2}$ and Zr $3d_{3/2}$ peaks,[49] unambiguously confirmed the presence of zirconium and elucidating its +4 oxidation states.[50] Fig. 4(c) illustrates the C 1s spectra, where identifying peaks corresponding to C═O, C–C, and C═C bonds, further confirmed the carbon framework's integrity.[51] Further, the deconvoluted O 1s spectrum (Fig. 4(d)) highlights the presence of distinct oxygen-related bonds, including C═O, C–O, and Zr–O, which reflect the diverse chemical environment of oxygen within the UiO-67 structure.[52]

3.2. Electrochemical studies

Cyclic Voltammetry (CV) studies were conducted using both bare and UiO-67-modified Glassy Carbon Electrodes (GCE) in a 0.1 M citrate buffer solution at a scan rate of 25 mV s^{-1}, both in the presence and absence of the analyte, Cadmium. Notably, the potential difference decreased significantly from 390 mV in the bare GCE to 109.2 mV after modification with UiO-67. This reduction in potential difference indicates enhanced electron transfer kinetics, as a higher potential difference typically corresponds to slower electron transfer, highlighting the enhanced electrocatalytic behaviour of the UiO-67-modified electrode. Furthermore, in the presence of cadmium ions, the bare GCE did not exhibit any discernible redox peaks, whereas the UiO-67-coated GCE showed notable variations, highlighting its improved sensitivity and detection capability, as depicted in Fig. 5(a and b).

To enhance the sensitivity of cadmium ion detection, Differential Pulse Voltammetry (DPV) was employed, as shown in Fig. 6(a). The DPV technique offers higher sensitivity and better resolution compared to cyclic voltammetry by applying a series of potential pulses superimposed on a linear potential ramp, which helps distinguish between closely spaced redox processes. This makes DPV particularly suitable for detecting trace levels of cadmium ions. A systematic pH optimization study was carried out over a range from 4 to 9 to identify the pH conditions that would provide the maximum electrochemical response as shown in Fig. 6(b).

The results indicated that a pH of 6 yielded the most favourable response. The enhanced current observed at pH 6 can be attributed to electrostatic interactions between the analyte (Cd^{2+} ions) and the UiO-67-modified glassy carbon electrode (GCE). In this range, the surface charge of the electrode and the ionization state of both the analyte and the UiO-67 material promote stronger electrostatic attraction, facilitating greater accumulation of cadmium ions at the electrode surface and thereby increasing the current response. However, beyond pH 6, a noticeable reduction of current was observed. This might be due to the hydrolysis of cadmium ions, which can occur at higher pH levels. Hydrolysis leads to the formation of cadmium hydroxide species, which are less electroactive and may precipitate, resulting in decreased availability of free cadmium ions for the redox process. Thus, the electrochemical signal weakens as the pH increases beyond the optimal value. Based on these findings, a 0.1 M citrate buffer at pH 6 was chosen as the optimal medium for cadmium ion detection.

Fig. 7(a) illustrates the concentration studies for cadmium (Cd^{2+}) ions. The observed increase in current with rising cadmium concentration could be attributed to the higher availability of electroactive species, enhancing electron transfer at the electrode surface. Additionally, the peak shifts toward more negative potentials as the concentration increases, likely due to changes in the mass transport or kinetic parameters and

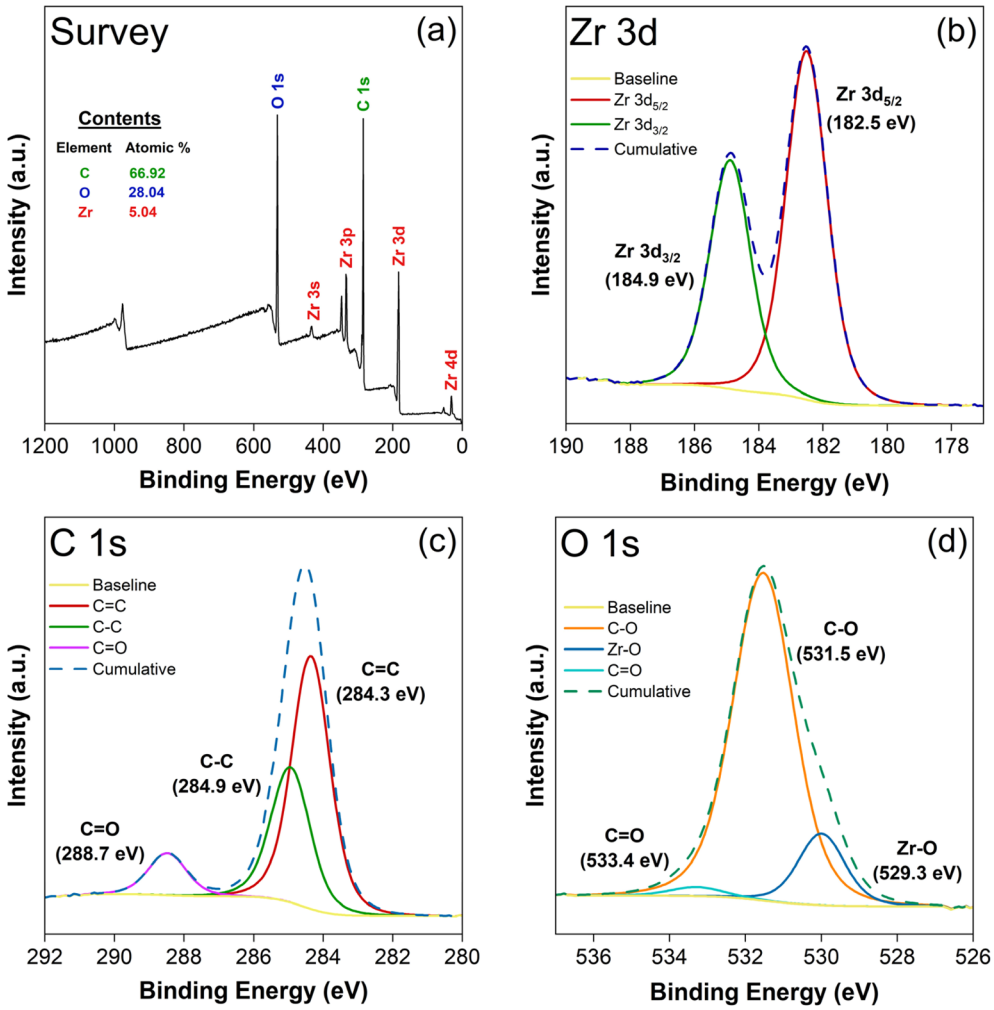

Fig. 4 XPS spectra of UiO-67: (a) survey spectrum; (b) Zr spectra; (c) C 1s spectra; (d) O 1s spectra.

electrode interface of the electrochemical reaction. Although the sensitivity of the detection method, with a sensitivity factor of 3.008 μA nM^{-1}, is moderate, it is still sufficient to achieve a low Limit of Detection (LoD) of 1.43 nM μA^{-1}, calculated using the formula: "LoD = (3.3 × standard deviation)/slope of the calibration curve". Similarly, the Limit of Quantification (LoQ)

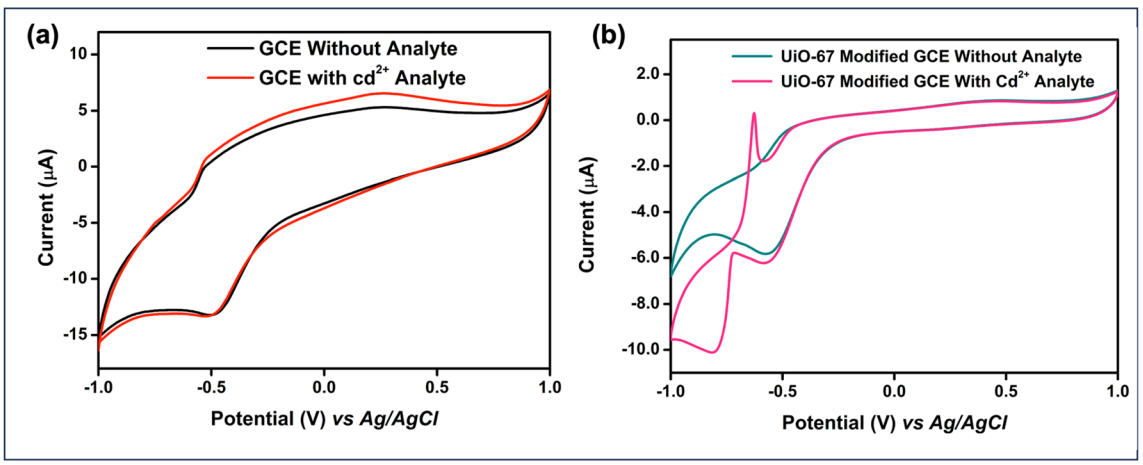

Fig. 5 Electrochemical behaviour of (a) bare GCE and (b) UiO-67 modified GCE.

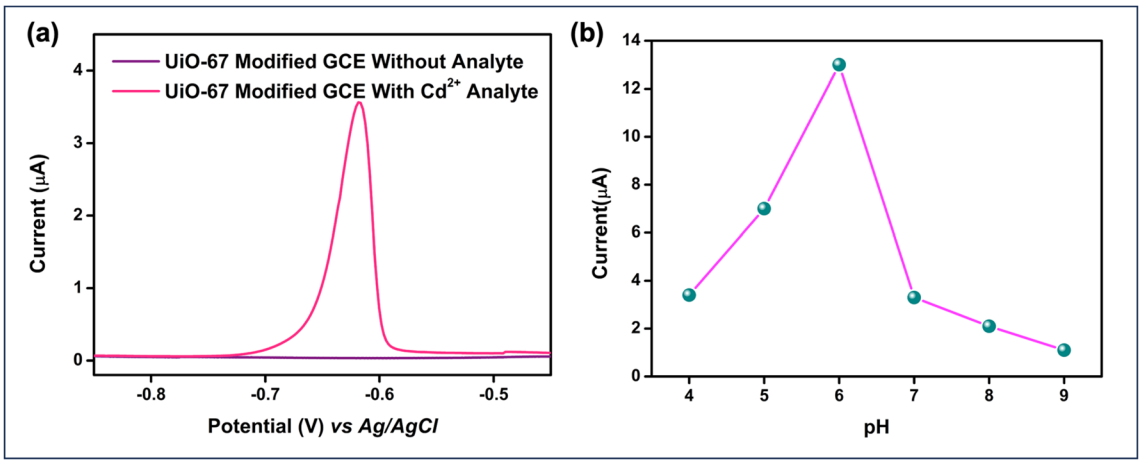

Fig. 6 DPV studies of (a) UiO-67 modified GCE and (b) pH calibration studies.

was found to be 4.34 nM μA^{-1}, based on the formula: "LoQ = (10 × standard deviation)/slope of the calibration curve". These values highlight the sensitivity and reliability of the detection method for cadmium ions, allowing for precise quantification even at low concentrations. These parameters indicate that the UiO-67-modified electrode is capable of detecting cadmium ions at trace levels, demonstrating its reliability and potential use in applications.

Typically, the response of a modified electrode to an analyte may be reduced after multiple measurements. In this study, the repeatability of the UiO-67-modified electrode for cadmium detection by continuously monitoring the electrochemical response of a 100 nM cadmium solution, as shown in Fig. 8(a). The consistent electrochemical responses observed across these measurements highlight the excellent repeatability and reliability of the UiO-67-based sensor for cadmium detection. Reproducibility was assessed by preparing three separate electrodes, each coated with UiO-67 MOF according to the same synthesis protocol. The sensors exhibited minimal variation in performance across different electrodes, confirming their good reproducibility and consistency as shown in Fig. 8(b). This low deviation highlights the reliability of the UiO-67 MOF-based sensor in delivering consistent results. Selectivity tests were conducted to evaluate the performance of the UiO-67-modified electrode against various metal ions, including Ni, Cd, Pb, Cu, and Zn. Among these ions, cadmium exhibited the most significant and consistent response, highlighting the sensor's superior selectivity for cadmium detection compared to the other metal ions as depicted in Fig. 8(c). The operational stability of the developed electrode was evaluated in the presence of 10 μM cadmium over 45 days, during which it maintained a sensitivity of 74.2%, indicating that the sensor can maintain its electrochemical activity over extended periods. Throughout the study, no significant peeling or delamination of the UiO-67 coating was observed, even after repeated immersion in the electrolyte solution. This suggests that the coating adheres well to the GCE surface and remains mechanically intact under normal operating conditions.

The comparison of existing UiO-67 electrochemical sensors is detailed in Table 1, illustrating its applicability across various

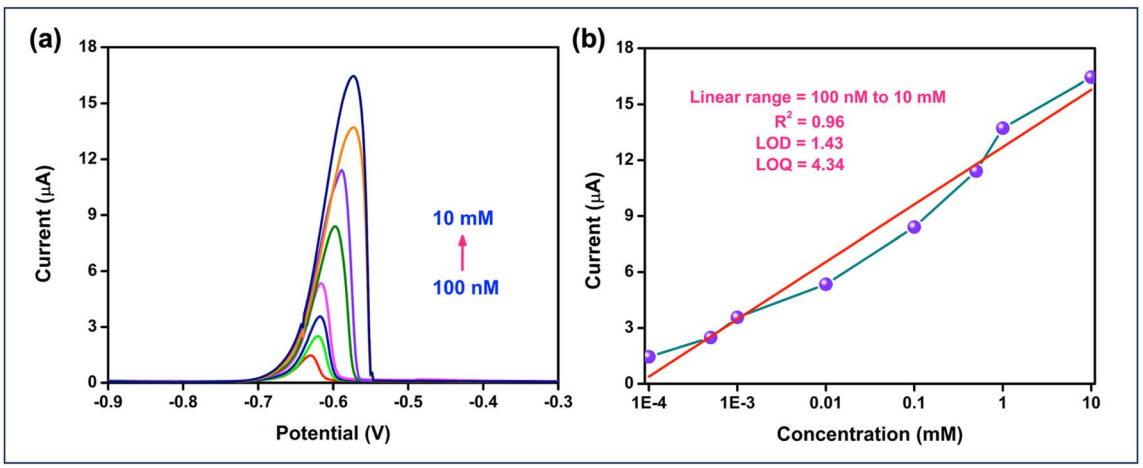

Fig. 7 (a) Concentration studies (b) linear calibration plot of Cd^{2+} ions.

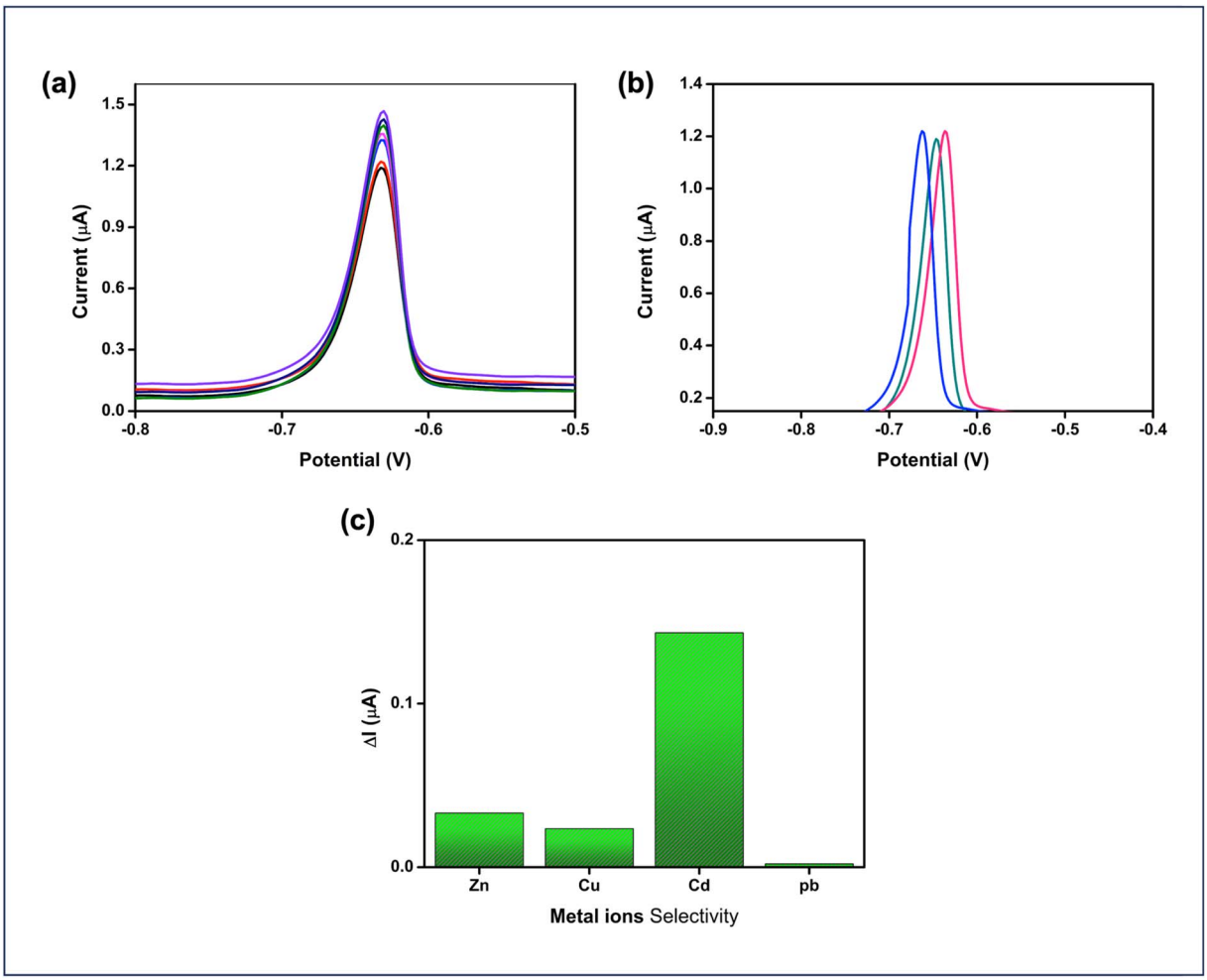

Fig. 8 (a) Repeatability, (b) reproducibility of 100 nM concentration Cd^{2+} analyte and (c) stability analysis for Cd^{2+} ions at a 500 nM concentration.

Table 1 Comparison of UiO-67 MOFs modified electrode with reported literature

Modified material	Analyte	Method	Detection limit (nM)	Ref.
UiO-67	Hydroquinone	DPV	3.5	35
GO/UiO-67@PtNPs	AS(III)	CV	0.48	32
Fe@UiO-67-BDA/GCE	Hg(II)	DPV	1.642	53
UiO-67	Cd(II)	DPV	1.43	Current work

scenarios. However, the detection of cadmium using UiO-67 has seldom been reported in the literature, indicating a significant research gap. This study addresses this gap by demonstrating the effectiveness of UiO-67 for cadmium detection, thereby contributing valuable insights to the field of environmental monitoring. Ultimately, our findings highlight the potential of UiO-67 as a reliable material for detecting cadmium contamination.

4. Conclusion

In this study, UiO-67 metal–organic framework was successfully synthesized using the solvothermal method. The effective synthesis was confirmed while preserving the structural integrity of the framework by the use of extensive characterisation techniques such as SEM, XRD, and FTIR. The UiO-67-modified Glassy Carbon Electrode (GCE) demonstrated a significant reduction in potential difference from 390 mV to 109.2 mV, and enhanced electrocatalytic behaviour, resulting in improved detection capabilities for cadmium ions (Cd^{2+}). The sensor achieved a low Limit of Detection (LoD) of 1.43 nM μA^{-1}, along with good repeatability and stability, highlighting its reliability for practical applications. These findings establish the UiO-67-modified GCE as a promising platform for heavy metal ion detection. Future research could explore further

functionalization of the UiO-67 framework to extend its applicability to a broader range of analytes in environmental monitoring and related fields.

Data availability

All relevant data pertaining to this work are mentioned in the manuscript itself.

Author contributions

Bhuvaneswari Selvaraj: data curation, investigation, writing – original draft, writing – review & editing. Lakshmi Priya G: conceptualization, writing – review & editing, supervision, investigation, funding acquisition. Selva Balasubramanian: formal analysis, writing – review & editing.

Conflicts of interest

The authors declare that they have no known competing financial interests or personal relationships that could have appeared to influence the work reported in this paper.

Acknowledgements

Authors are much thankful to acknowledge the support of Vellore Institute of Technology, Chennai Campus, for the experimental research work, open-access publication, and the post-doctoral fellowship awarded to the author Bhuvaneswari Selvaraj.

References

1 S. N. Zulkifli, H. A. Rahim and W.-J. Lau, *Sens. Actuators, B*, 2018, **255**, 2657–2689.
2 A. Boretti and L. Rosa, *npj Clean Water*, 2019, **2**, 15.
3 A. du Plessis, *One Earth*, 2022, **5**, 129–131.
4 D. Kadadou, L. Tizani, H. Alsafar and S. W. Hasan, *MethodsX*, 2024, **12**, 102582.
5 S. Das, K. W. Sultana, A. Ndhlala, M. Mondal and I. Chandra, *Environ. Health Insights*, 2023, **17**, DOI: **10.1177/11786302231201259**.
6 B. Bansod, T. Kumar, R. Thakur, S. Rana and I. Singh, *Biosens. Bioelectron.*, 2017, **94**, 443–455.
7 P. B. Tchounwou, C. G. Yedjou, A. K. Patlolla and D. J. Sutton, *Exper. Suppl.*, 2012, **101**, 133–164.
8 A. Saadati, F. Farshchi, M. Hasanzadeh, Y. Liu and F. Seidi, *RSC Adv.*, 2022, **12**, 21836–21850.
9 M. B. Gumpu, M. Veerapandian, U. M. Krishnan and J. B. B. Rayappan, *Talanta*, 2017, **162**, 574–582.
10 B. Bansod, T. Kumar, R. Thakur, S. Rana and I. Singh, *Biosens. Bioelectron.*, 2017, **94**, 443–455.
11 Q. Ding, C. Li, H. Wang, C. Xu and H. Kuang, *Chem. Commun.*, 2021, **57**, 7215–7231.
12 Y. Wei, C. Gao, F. L. Meng, H. H. Li, L. Wang, J. H. Liu and X. J. Huang, *J. Phys. Chem. C*, 2012, **116**, 1034–1041.
13 C. Venkateswara Raju, C. Hwan Cho, G. Mohana Rani, V. Manju, R. Umapathi, Y. Suk Huh and J. Pil Park, *Coord. Chem. Rev.*, 2023, **476**, 214920.
14 Q. Yang, X. Sun, Y. Sun, X. Shen and Y. Pang, *ACS Appl. Nano Mater.*, 2023, **6**, 7901–7909.
15 J. Jose, P. Prakash, B. Jeyaprabha, R. Abraham, R. M. Mathew, E. S. Zacharia, V. Thomas and J. Thomas, *J. Iran. Chem. Soc.*, 2023, **20**, 775–791.
16 C. X. Lü, G. P. Zhan, K. Chen, Z. K. Liu and C. D. Wu, *Appl. Catal. B Environ.*, 2020, **279**, DOI: **10.1016/j.apcatb.2020.119350**.
17 J. Ru, X. M. Wang, K. Li, X. G. Ma, T. Jiang, G. F. Sun, Y. Hu, Y. Li and X. Q. Lu, *Sep. Purif. Technol.*, 2024, **330**, DOI: **10.1016/j.seppur.2023.125454**.
18 X. Gong, Y. Bi, Y. Zhao, G. Liu and W. Y. Teoh, *RSC Adv.*, 2014, **4**, 24653–24657.
19 J. Milikić, M. Savić, A. Janošević Ležaić, B. Šljukić and G. Ćirić-Marjanović, *Polymers*, 2024, **16**(5), 683.
20 P. Dey, M. Kaur, A. Khajuria, D. Kaur, M. Singh, H. K. Alajangi, N. Singla, G. Singh and R. P. Barnwal, *Microchem. J.*, 2024, **196**, 109672.
21 S. S. Shafqat, M. Rizwan, M. Batool, S. R. Shafqat, G. Mustafa, T. Rasheed and M. N. Zafar, *Chemosphere*, 2023, **318**, 137920.
22 M. Devaraj, Y. Sasikumar, S. Rajendran and L. C. Ponce, *J. Electrochem. Soc.*, 2021, **168**, 037513.
23 N. Garg, A. Deep and A. L. Sharma, *Crit. Rev. Anal. Chem.*, 2022, 1–25.
24 J. H. Cavka, S. Jakobsen, U. Olsbye, N. Guillou, C. Lamberti, S. Bordiga and K. P. Lillerud, *J. Am. Chem. Soc.*, 2008, **130**, 13850–13851.
25 Y. Bai, Y. Dou, L.-H. Xie, W. Rutledge, J.-R. Li and H.-C. Zhou, *Chem. Soc. Rev.*, 2016, **45**, 2327–2367.
26 A. Schaate, P. Roy, A. Godt, J. Lippke, F. Waltz, M. Wiebcke and P. Behrens, *Chem.–Eur. J.*, 2011, **17**, 6643–6651.
27 J. Ru, X. Wang, F. Wang, X. Cui, X. Du and X. Lu, *Ecotoxicol. Environ. Saf.*, 2021, **208**, 111577.
28 A. H. Vahabi, F. Norouzi, E. Sheibani and M. Rahimi-Nasrabadi, *Coord. Chem. Rev.*, 2021, **445**(5), 214050.
29 D. K. Yoo and S. H. Jhung, *J. Mater. Chem. A*, 2022, **10**, 8856–8865.
30 K. Chattopadhyay, M. Mandal and D. K. Maiti, *Mater. Adv.*, 2023, **5**, 51–67.
31 Y. Q. Xiang, H. D. Yan, B. J. Zheng, A. Faheem, W. L. Chen and Y. G. Hu, *Chemosphere*, 2021, **270**, 128672.
32 J. Ru, X. Wang, J. Zhao, J. Yang, Z. Zhou, X. Du and X. Lu, *Microchem. J.*, 2022, **181**, 107765.
33 S. K. Mondal, P. O. Aina, A. A. Rownaghi and F. Rezaei, *Chem. Eng. J.*, 2024, **493**, 152269.
34 X. Dong, Y. Lin, Y. Ma and L. Zhao, *RSC Adv.*, 2019, **9**, 27674–27683.
35 T. Zhang, J. Z. Wei, X. J. Sun, X. J. Zhao, H. L. Tang, H. Yan and F. M. Zhang, *Inorg. Chem.*, 2020, **59**, 8827–8835.
36 S. Hu, S. Zhang, J. Qin, K. Cai, C. Peng, L. Luo, Y. Gu and Y. Mei, *Microchem. J.*, 2024, **205**, DOI: **10.1016/j.microc.2024.111154**.

37 G. A. Bodkhe, M. S. More, A. Umar, A. A. Ibrahim, S. Siva, M. A. Deshmukh, N. N. Ingle, D. K. Gaikwad, M. L. Tsai, T. Hianik, M. Kim and M. D. Shirsat, *J. Environ. Chem. Eng.*, 2024, **12**(3), DOI: **10.1016/j.jece.2024.113024**.
38 S. Verma, A. K. Sharma and S. K. Shukla, *Mater. Adv.*, 2023, **4**, 3521–3531.
39 A. B. Patil, P. L. Chaudhary and P. V. Adhyapak, *RSC Adv.*, 2024, **14**, 12923–12934.
40 A. Lochab, K. Jindal, A. Chowdhuri, M. Tomar and R. Saxena, *Microchem. J.*, 2024, **198**, DOI: **10.1016/j.microc.2024.110125**.
41 S. Øien, D. Wragg, H. Reinsch, S. Svelle, S. Bordiga, C. Lamberti and K. P. Lillerud, *Cryst. Growth Des.*, 2014, **14**, 5370–5372.
42 X. Dong, Y. Lin, Y. Ma and L. Zhao, *RSC Adv.*, 2019, **9**, 27674–27683.
43 S. Ghaedi, H. Rajabi, M. Hadi Mosleh, P. Babakhani and M. Sedighi, *J. Environ. Chem. Eng.*, 2024, **12**, 114511.
44 S. M. Masoom Nataj, S. Kaliaguine and F.-G. Fontaine, *ChemCatChem*, 2023, **15**, e202300079.
45 M. Yuen Ying, Z. M. Aljunid Merican, A. Haruna and S. G. Musa, *J. Sci. Technol.*, 2023, **6**, 2.
46 C. Zhao, Y. Cui, F. Fang, S. Ryu and J. Huang, *Adv. Condens. Matter Phys.*, 2017, **2017**, 1–8.
47 A. H. Vahabi, F. Norouzi, E. Sheibani and M. Rahimi-Nasrabadi, *Coord. Chem. Rev.*, 2021, **445**, 214050.
48 S. K. Mondal, P. O. Aina, A. A. Rownaghi and F. Rezaei, *Chem. Eng. J.*, 2024, **493**, 152269.
49 R. Nie, C. Yang, J. Zhang, K. Dong and G. Zhao, *Water Sci. Technol.*, 2021, **84**, 1594–1607.
50 J. Tang, X. Ma, J. He, X. Liu and M. Li, *J. Environ. Chem. Eng.*, 2022, **10**, 107820.
51 X. Wang, W. Sun, Y. Tian, K. Dang, Q. Zhang, Z. Shen and S. Zhan, *Small*, 2021, **17**, 2100367.
52 Y. Qiang, W. Yang, X. Zhang, X. Luo, W. Tang, T. Yue and Z. Li, *Microchim. Acta*, 2022, **189**(3), DOI: **10.1007/s00604-022-05236-2**.
53 T. Si-Yu, D. Zhu, Y. Mu-Lan, L. Si-Mian, H. Xiang-Yang, T. Long, Y. Er-Lin, W. Xiao and W. Ji-Jiang, *Microchem. J.*, 2024, **206**, 111670.